

Optical refrigeration of the Yb^{3+} -doped YAG crystal close to the thermoelectric cooling limit

Cite as: Appl. Phys. Lett. **118**, 131104 (2021); <https://doi.org/10.1063/5.0047086>

Submitted: 10 February 2021 • Accepted: 13 March 2021 • Published Online: 29 March 2021

 Biao Zhong, Yongqing Lei, Xuelu Duan, et al.



View Online



Export Citation



CrossMark

ARTICLES YOU MAY BE INTERESTED IN

[Bright room temperature near-infrared single-photon emission from single point defects in the AlGaIn film](#)

Applied Physics Letters **118**, 131103 (2021); <https://doi.org/10.1063/5.0045506>

[Classical-to-topological transmission line couplers](#)

Applied Physics Letters **118**, 131102 (2021); <https://doi.org/10.1063/5.0041055>

[Optical gain and absorption of 1.55 \$\mu\text{m}\$ InAs quantum dash lasers on silicon substrate](#)

Applied Physics Letters **118**, 131101 (2021); <https://doi.org/10.1063/5.0043815>

 QBLOX



1 qubit

Shorten Setup Time

Auto-Calibration
More Qubits

Fully-integrated

Quantum Control Stacks
Ultrastable DC to 18.5 GHz
Synchronized <<1 ns
Ultralow noise



100s qubits

[visit our website >](#)

Optical refrigeration of the Yb^{3+} -doped YAG crystal close to the thermoelectric cooling limit

Cite as: Appl. Phys. Lett. **118**, 131104 (2021); doi: [10.1063/5.0047086](https://doi.org/10.1063/5.0047086)

Submitted: 10 February 2021 · Accepted: 13 March 2021 ·

Published Online: 29 March 2021



View Online



Export Citation



CrossMark

Biao Zhong,^{1,a)}  Yongqing Lei,¹ Xuelu Duan,¹ Tao Yang,^{1,2,a)}  and Jianping Yin^{1,a)}

AFFILIATIONS

¹State Key Laboratory of Precision Spectroscopy, East China Normal University, Shanghai 200062, People's Republic of China

²Collaborative Innovation Center of Extreme Optics, Shanxi University, Taiyuan, Shanxi 030006, People's Republic of China

^{a)}Authors to whom correspondence should be addressed: bzhong@lps.ecnu.edu.cn; tyang@lps.ecnu.edu.cn; and jpyin@phy.ecnu.edu.cn

ABSTRACT

The Yb^{3+} :YAG crystal has been one of the most widely used active media in the solid-state lasers of high power, mainly thanks to its excellent thermal, mechanical, and optical properties. Thermal effect due to heat deposition in the active medium, however, greatly deteriorates the beam quality of the laser output and sets a limit on its maximum power available. Although the cooling proposal of anti-Stokes fluorescence can help realize the heat-free high-power lasers with good beam quality, so-called radiation-balanced lasers, there is no substantial advancement in the optical cooling of Yb^{3+} :YAG crystals since its latest experimental report with a temperature drop of about 9 K. Here we demonstrate experimentally a remarkable temperature drop of about 80 K in a 3% Yb^{3+} -doped YAG single crystal pumped by a fiber laser at 1030 nm. Further analysis predicts that the cooling limit of the titled crystal can reach as low as 180 K from the room temperature. Our work therefore reveals a key pathway to facilitate the optical refrigeration of the Yb^{3+} :YAG crystal down to the thermoelectric cooling limit, thus offering a unique entry point to practical radiation-balanced lasers.

Published under license by AIP Publishing. <https://doi.org/10.1063/5.0047086>

Optical cooling of solids via anti-Stokes fluorescence was initially proposed by P. Pringsheim in 1929¹ and later demonstrated experimentally by Epstein *et al.* in 1995.² Since then, extensive advances have been made in the Yb^{3+} -, Tm^{3+} -, Er^{3+} -, and Ho^{3+} -doped bulky crystals and glasses,^{3–18} as well as in the nano-crystals and semiconductors.^{19–22} Anti-Stokes fluorescence cooling can be employed to develop vibration-free cryogenic optical coolers,^{2,9,23} and it is even expected to solve the problem of thermal deposition in the gain medium of solid-state lasers.^{24–27} Solid-state lasers with high output power and good beam quality are highly desirable in industry and science fields, whose gain media are mainly crystals or glasses doped with lanthanide or transition metal ions.^{28–32} Due to its excellent properties, such as high thermal conductivity and physical hardness, as well as large absorption bandwidth and low values of intrinsic non-radiative losses for diode pumpers,^{33,34} Yb^{3+} :YAG (Yttrium aluminum garnet, $\text{Y}_3\text{Al}_5\text{O}_{12}$) crystal has been one of the most widely used active media in both optical coolers and solid-state lasers.^{26,27,34–40}

Thermal deposition can cause thermal gradient inside the gain medium and result in unwanted thermal effects during laser operation, which not only affects the laser coherence, polarization, and stability but also hinders the production of high laser power.^{41–43} Various

methods have been developed to deal with this fundamental problem, however, even with advanced thermal management schemes, the residual thermal effect still deteriorates the beam quality and ultimately limits the high-power production.^{43,44} Bowman first proposed that the heat deposited in the laser gain medium can be taken away by the fluorescent radiation and thus realize the heat-free-state laser operation, which he nominated as radiation-balanced lasers (RBLs) or athermal lasers.^{45,46} Recently, Yang *et al.* demonstrated an RBL in an intracavity-pumped Yb^{3+} :YAG crystal disk and introduced a roadmap for developing disk RBLs of kilowatt power with high beam quality and minimal adverse thermal degradation.^{35,47} According to the theoretical model of laser cooling, the Yb^{3+} :YAG crystal can be further cooled to ~ 138 K.^{37,48} However, no further experiments have been carried out ever since.

In this work, we cooled the 3% Yb^{3+} :YAG crystal and obtained a temperature drop of about 80 K utilizing a 1030 nm CW fiber laser of 36 W. Exploiting the experimental parameters such as external quantum efficiency, background absorption coefficient, and mean fluorescence wavelength, we further obtain the cooling window of the 3% Yb^{3+} -doped YAG crystal via the four-energy-level model, and predict that the minimum available temperature of the titled crystal can reach

as low as 180 K without further purification. Compared to the temperature drop of about 9 K reported in the latest experimental works,^{34,36} our results reveal a key pathway to facilitate the optical cooling of the Yb³⁺:YAG crystal down to the thermoelectric cooling limit, thus offering a unique entry point to practical RBLs.

High-purity Yb³⁺-doped YAG crystals investigated here were grown by using the Czochralski method.⁴⁹ YAG is one of the synthetic crystalline materials of the garnet group, which has a cubic yttrium aluminum oxide phase. Figure 1(a) describes the absorption and emission spectra of the 3% Yb³⁺:YAG crystal at 300 K. The red dash line and the blue shaded region denote the mean fluorescence wavelength $\lambda_f(300\text{ K}) = 1011.6\text{ nm}$ and the cooling tail at 300 K, respectively. When the Yb³⁺ ions are doped in the YAG host, the ²F_{7/2} and ²F_{5/2} levels of the Yb³⁺ ions will be split into four and three Stark sublevels, respectively, since the point symmetry of the host is getting lower than the cubic one.²³ The inset in Fig. 1(a) shows the energy levels of the ground-state ²F_{7/2} and the excited state ²F_{5/2} with seven Stark manifolds (E1–E7). The ground state Yb³⁺ ions doped in YAG crystal are pumped to the excited state by absorbing photons of wavelength λ_p . After thermalization via phonon absorption from the host, the excited Yb³⁺ ions decay spontaneously to the ground state emitting fluorescence photons. The energy difference between the excitation and average fluorescence photons is on the order of a few $k_B T$.⁵⁰

The cooling efficiency of the rare-earth-ion doped glass/crystal can be expressed as:⁵¹ $\eta_c = 1 - \eta_{ext}\eta_{abs}\frac{\lambda_p}{\lambda_f}$, where $\eta_{ext} = \eta_e W_r / (\eta_e W_r + W_{nr})$ and $\eta_{abs} = \alpha_r / (\alpha_r + \alpha_b)$ are the external quantum and the absorption efficiency, respectively. Here η_e is the fluorescence extraction efficiency, while W_r and W_{nr} indicate the radiation and non-radiation recombination rates, respectively. In addition, α_r and α_b represent the resonance and background absorption coefficients, respectively. For the Yb³⁺-doped system with an energy gap of about 10000 cm⁻¹ between the ground and excited states, $\eta_{ext}\eta_{abs} > 98\%$ is required for achieving net cooling.^{50,52} Efficient laser cooling generally requires $\hbar\omega_{max} < E_p/8$, with E_p being the energy gap of the ion quantum states involved in the laser cooling process and $\hbar\omega_{max}$ the phonon energy of the host material. Fortunately, the maximum phonon energy $\hbar\omega_{max}$ of Yb³⁺:YAG crystal is only about 700 cm⁻¹ and meet such a criterion.³³

The emission fluorescence spectra of the 3% Yb³⁺:YAG crystal sample pumped by the CW laser of 1 mW at 914 nm were measured

at temperatures of 80 K–300 K with an interval of 10 K by utilizing the thermostat (Janis VPF-100). Figure 1(b) selectively shows a few of the measured fluorescence spectra, indicating two peaks appearing at 1030 nm and 1048 nm larger than the mean fluorescence wavelength λ_f . Here, λ_f can be obtained from the emission fluorescence spectra according to the formula $\lambda_f = \int \lambda S(\lambda, T) d\lambda / \int S(\lambda, T) d\lambda$, where $S(\lambda, T)$ is the temperature-dependent emission spectrum of the sample. The inset in Fig. 1(b) shows the linear dependence of λ_f on the temperature of the sample measured in the experiment as $\lambda_f = 1031.2 - 0.066 \times T$ (nm).

The schematic diagram of the experiment is shown in Fig. 2(a). The Yb³⁺-doped YAG crystal sample with dimensions of 2 × 2 × 5 mm³ was placed inside a vacuum chamber of pressure about 1 × 10⁻⁴ Pa and irradiated by a fiber laser (PreciLasers YFL-1020–50) beam with a varying wavelength from 1010 nm to 1080 nm. The front and rear surfaces of the sample were highly polished and cut at Brewster angles. The maximum laser power incident onto the crystal was measured to be 36 W at 1030 nm. The sample was placed on two fibers of diameter 100 μm , which were further supported by two pairs of steel rods. The windows of the vacuum chamber were anti-reflection coated in the wavelength range from 980 nm to 1080 nm. The fluorescence was collected by a multimode fiber of diameter 600 μm and transported to a spectrometer (Ocean Optics: Maya 2000Pro). The temperature of the crystal was measured by the method of non-contact DLT.⁵¹ The temperature of the sample got stabilized after about 10 min of laser irradiation, indicating the cooling power of the crystal sample balances with the heat load from the environment. The convective heat load from the residual gas in the high vacuum chamber and the heat load from contact with the fibers can be ignored. The radiative heat load mainly comes from the blackbody radiation of the environment.

A laser-induced thermal modulation spectroscopy (LITMoS) test measurement of the 3% Yb³⁺-doped YAG crystal at the room temperature with the tunable fiber laser has also been performed. The corresponding experimental data and fitting line are shown in Fig. 2(b). The best fit to data, $\eta_{ext} = 0.992$ and $\alpha_b = 1.5 \times 10^{-4}\text{ cm}^{-1}$ are obtained. Figure 2(c) illustrates the absorption spectra of the 3% Yb³⁺:YAG crystal with a temperature interval of 50 K, which were calculated by the reciprocity method⁵³ from the fluorescence spectra shown in Fig. 1(b). Absorption peaks at the wavelength of 1030 nm

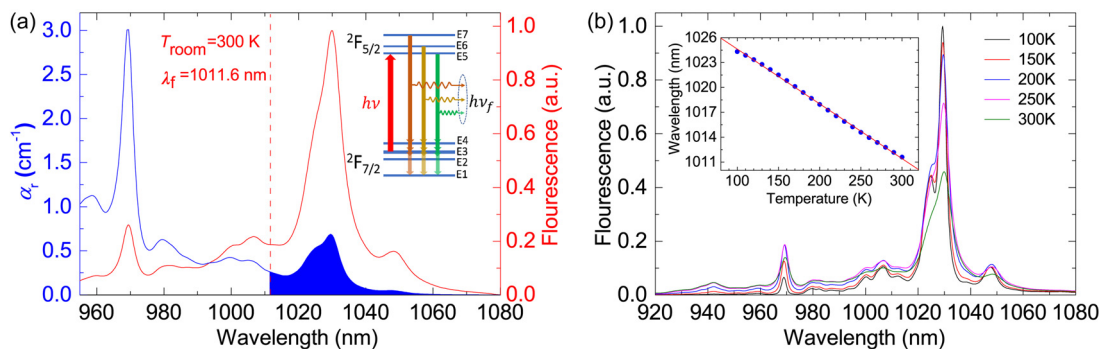


FIG. 1. (a) Absorption spectra (blue line) and emission spectra (red line) of 3% Yb³⁺-doped in YAG crystal at the temperature of 300 K, where the dash line and the blue shaded region denote the mean fluorescence wavelength and the cooling tail, respectively. The inset indicates the anti-Stokes fluorescence cooling process in the Yb³⁺:YAG crystal. (b) Temperature-dependent fluorescence spectra of Yb³⁺:YAG crystal normalized by integrated value at 100 K; the inset shows temperature dependence of the mean fluorescence wavelength along with an approximate linear fit in the temperature range of 100 K–300 K.

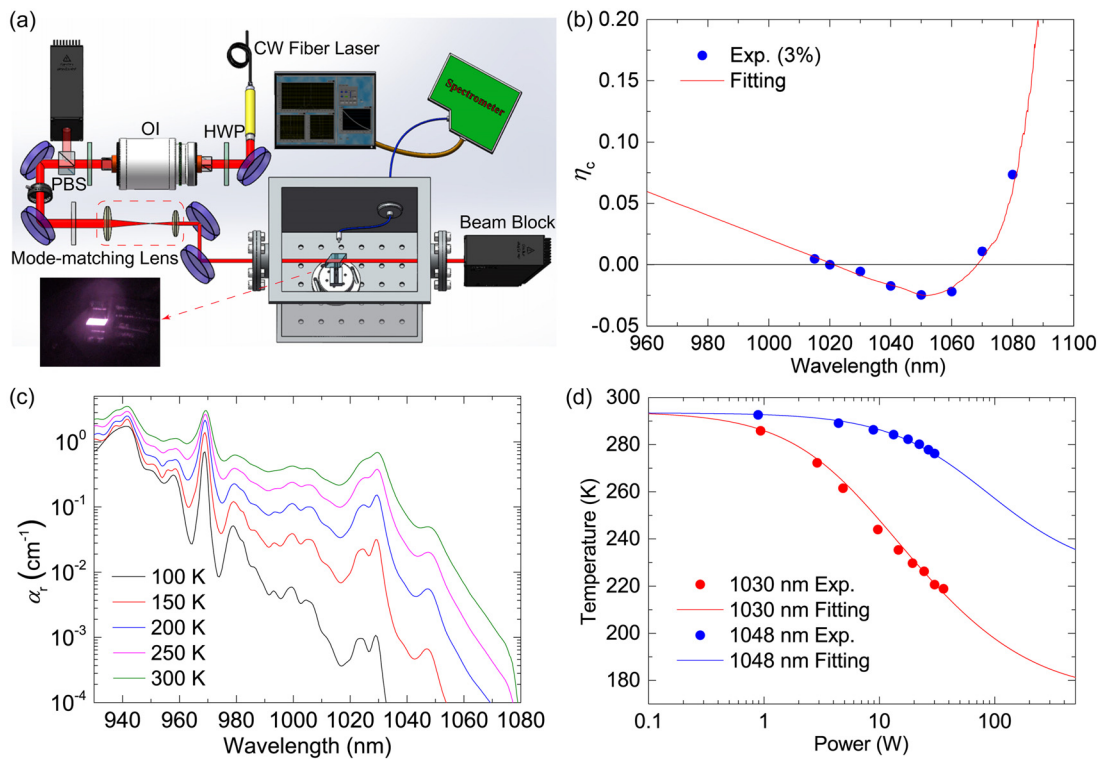


FIG. 2. (a) Experimental schematics of the single-pass optical cooling setup. (b) LITMoS test result for 3% Yb^{3+} -YAG crystal. (c) Temperature-dependent absorption spectra of 3% Yb^{3+} -YAG crystal with an interval of 50 K. (d) The temperature dependence of the 3% Yb^{3+} -doped YAG crystal on the pump power of the laser at 1030 and 1048 nm, respectively.

and 1048 nm correspond to resonant transitions of E3–E5 and E4–E5, respectively, as shown in Fig. 1(a). As one can obtain from both the absorption [Fig. 2(c)] and fluorescence [Fig. 1(b)] spectra, there are two peaks appearing at 1030 nm and 1048 nm that are suitable for achieving optimal cooling effect, which can be further supported by our following experimental and simulation results. Figure 2(d) shows the dependence of the temperature of the 3% Yb^{3+} -doped YAG crystal sample on the laser power when pumped at a wavelength of 1030 nm (red line) and 1048 nm (blue line), respectively. The overall cooling effect was found to be the best when the sample was pumped at a wavelength of 1030 nm, at which both the absorption and the fluorescence emission of the crystal sample have a local maximum intensity. When the temperature of the crystal sample gets stabilized, the cooling power of the sample $P_{cool} = P_{pump}(1 - \exp[-\alpha l])\eta_c$ equals the radiative heat load of the blackbody radiation from the environment $P_{rad} = \sigma_B A_s \varepsilon_s (T_r^4 - T^4)/(1 + \chi)$.⁵³ And the conductive heat load from the supporting fiber with a diameter of 100 μm held by four aluminum posts of 1.5 mm diameter $P_{cot} = C_f(T_r - T)$. Here, P_{pump} is the pump laser power, α and l are the absorption coefficient and the length of the crystal, σ_B is the Stefan–Boltzmann constant, T_r and T are the temperatures of the environment and the crystal sample, respectively, and $\chi = (1 - \varepsilon_e)\varepsilon_s A_s / \varepsilon_e A_e$ with A and ε being the corresponding surface and the thermal emissivity. The subscripts s and e denote the sample and the environment (vacuum chamber), respectively. Here, $C_f \approx 34.8 \mu\text{W/K}$ is adopted. In Fig. 2(d), the solid lines

are fitted according to equation of $P_{cool} = P_{rad} + P_{cot}$. The parameters η_{ext} of 0.992 and α_b of $1.5 \times 10^{-4} \text{cm}^{-1}$ for both wavelengths are employed in the fitting process of the LITMoS test. With $P_{pump} = 36 \text{ W}$ at 1030 nm, the sample was optically cooled down to the temperature of 218.9 K in our experiment. With the calculated absorption power of about 3.41 W and the cooling power P_{cool} of 14.1 mW, the cooling efficiency was found to be about -0.4% . An extrapolation of the fitting curve at 1030 nm indicates that the lowest temperature of this crystal can approach below 200 K.

The dependence of the cooling effect of the sample on the pump laser wavelength in the cooling tail was also investigated and the corresponding results are shown by the solid shots in Fig. 3, which implies that the best cooling effect was obtained at the pump laser wavelength of 1030 nm. As mentioned above, the sample has an absorption peak at 1030 nm in the cooling tail corresponding to the resonance transition from E3 to E5. When the sample was pumped at a wavelength larger than 1030 nm, the energy difference between the pump laser photon and the average fluorescence photon became larger such that more heat could be carried away. However, due to the rapid decline in absorption, the real cooling effect is even worse than that at 1030 nm.

The relationship between the cooling effect and the pump laser wavelength could be delineated clearly from the so-called “cooling window,” which characterizes the refrigeration capabilities of the crystal pumped at different laser wavelengths and temperatures.⁵¹ We calculated the cooling window of the 3% Yb^{3+} -doped YAG crystal with

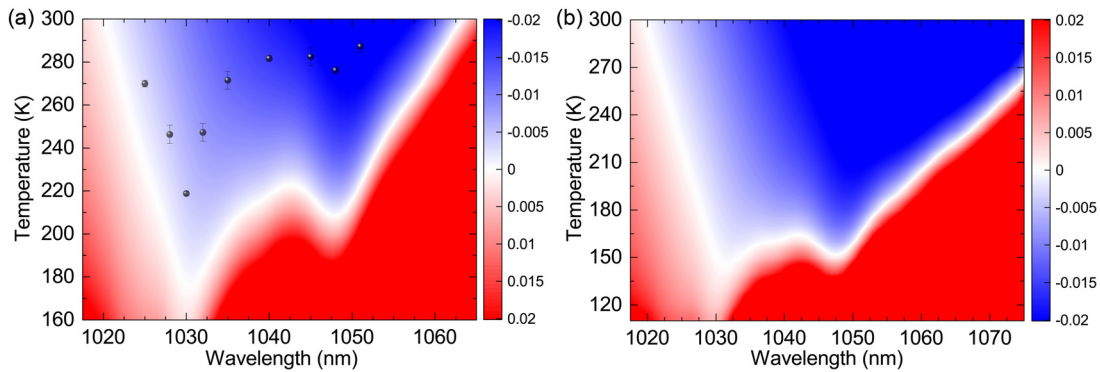


FIG. 3. The cooling window of the 3% Yb^{3+} -doped YAG crystal, which describes the dependence of the cooling efficiency on the crystal temperature and the pump laser wavelength. The blue and red regions denote cooling and heating, respectively. (a) The global minimum achievable temperature of the sample (pumped at 1030 nm) is calculated to be 180 K ($\alpha_b = 1.5 \times 10^{-4} \text{ cm}^{-1}$). The blue solid circles with an error bar represent the final temperature of the crystal after irradiated by the pump laser of about ~ 36 W at different wavelengths. (b) The global minimum achievable temperature of the sample with the $\alpha_b = 1.5 \times 10^{-5} \text{ cm}^{-1}$ (pumped at 1030 nm) is calculated to be about 145 K.

the external quantum efficiency $\eta_{\text{ext}} = 0.992$ and background absorption coefficient $\alpha_b = 1.5 \times 10^{-4} \text{ cm}^{-1}$, which were obtained by fitting the experimental data. As shown in Fig. 3(a), the cooling window indicates that the crystal sample can be potentially cooled to a temperature of about 180 K at a pump wavelength of 1030 nm. If we further improve the purity of the crystal and reduce the background absorption coefficient of the sample to $\alpha_b = 1.5 \times 10^{-5} \text{ cm}^{-1}$, then the global minimum achievable temperature of the sample can reach 145 K at the pump wavelength of 1030 nm according to the cooling window in Fig. 3(b). Therefore, it might be a good starting point to pump the Yb^{3+} -doped YAG crystal at 1030 nm when using it as the gain medium of RBLs. Although the YAG crystal has a relatively high refractive index (~ 1.83), which is not favorable for fluorescence photons to escape, this issue can still be resolved by appropriately shaping the geometry of the YAG crystal such as a disk. We also notice that the minimum achievable temperature of the Yb^{3+} -doped YAG crystal is higher than that of the Yb^{3+} -doped fluoride crystals,⁵³ however, the high thermal conductivity, ruggedness as well as the excellent gain media performance make the Yb^{3+} -doped YAG crystal an attractive material for wide use in the RBLs.

In previous studies, Epstein *et al.*³⁴ realized a temperature drop of ~ 8.9 K in a 2.3% Yb^{3+} :YAG crystal placed in the vacuum chamber of 1.33×10^{-4} Pa, with the absorbed pump power P_{abs} by the crystal being about 1.8 W, the background absorption coefficient of the sample α_b being $2.2 \times 10^{-4} \text{ cm}^{-1}$, and the mean emission fluorescence wavelength λ_f being 995 nm. In contrast, de Lima Filho *et al.*³⁶ reported a temperature drop of ~ 8.8 K in a 3% Yb^{3+} :YAG crystal of $1 \times 1 \times 10 \text{ mm}^3$ in air, with P_{abs} being about 1.0 W, α_b being $2.89 \times 10^{-4} \text{ cm}^{-1}$, η_{ext} being 0.991 and λ_f being 1010 nm. They claimed that the discrepancies arise from the geometries of the samples, whose crystal is closed to having the optimum dimensions that is derived from the simulation. Although reducing the cross section of the sample implies smaller potential thermal load, smaller probability of fluorescence re-absorption and lower achievable temperature, the radius of the pump laser beam sets an upper limit of the sample's cross section since the amount of the absorbed pump power that cools the sample is also limited. In our experiment, the temperature drop of ~ 80 K was achieved in the 3% Yb^{3+} :YAG crystal of $2 \times 2 \times 5 \text{ mm}^3$ in

a vacuum environment of 1×10^{-4} Pa. The absorbed pump power has been calculated to be about 3.4 W in our setup, with α_b being $1.5 \times 10^{-4} \text{ cm}^{-1}$, η_{ext} being 0.992 and λ_f being 1011.6 nm. While the difference between the mean emission fluorescence wavelengths of the two crystals is trivial, the dramatic temperature drop in our experiment is mainly ascribed to the enhancement in the crystal quality (as shown by the reduced value of α_b), the increase in the absorbed pump power and the improvement in the heat load management. A more recent work by Yang *et al.*³⁵ revealed that a RBL in a 5% Yb^{3+} :YAG crystal disk at the room temperature, with α_b being $3 \times 10^{-3} \text{ cm}^{-1}$, η_{ext} being 0.996 and λ_f being 1019 nm. The authors aimed to build a demo RBL in which the exothermic quantum defect balances with the endothermic spontaneous emission such that the disk stabilizes at the room temperature.

To conclude, we have experimentally explored the cooling potential of the Yb^{3+} -doped YAG crystal irradiated by a CW fiber laser. With a laser power of 36 W at 1030 nm, a 3% Yb^{3+} -doped YAG crystal sample of volume $2 \times 2 \times 5 \text{ mm}^3$ was optically cooled from room temperature down to 218.9 K with temperature drop of about 80 K in the vacuum environment. The cooling power of the sample was calculated to be about 14.1 mW with the corresponding cooling efficiency being about 0.6%. Simulation based on our experimental results indicates that the current 3% Yb^{3+} -doped YAG sample can be potentially cooled down to the thermoelectric cooling limit of 180 K. If the crystal sample is further purified with the background absorption coefficient reduced to $\alpha_b = 1.5 \times 10^{-5} \text{ cm}^{-1}$, its achievable temperature can be even reduced to about 145 K when pumped at 1030 nm. Our work here not only provides a solid evidence that laser cooling of Yb^{3+} :YAG crystal could be a suitable method for developing practical RBLs of high power, but also broadens our understanding about the metal ion-doped crystals in an all-solid-state optical refrigeration application.

AUTHORS' CONTRIBUTIONS

B.Z. and Y.L. equally contributed to this work.

We thank Professor M. Sheik-Bahae (University of New Mexico), Professor M. Tonelli (Università di Pisa), Dr. A. Gragossian (University of New Mexico), Dr. Z. Yang (University of

New Mexico), Dr. J. W. Meng (University of New Mexico) for helpful discussions. Biao Zhong thanks Dr. L. Z. Deng (East China Normal University) for his generous help. This work is partially supported by the Fundamental Research Funds for the Central Universities, the National Natural Science Foundation of China (Grant Nos. 11604100, 11834003, 61574056, 91536218, and 11874151), the Program for Professor of Special Appointment (Eastern Scholar) at Shanghai Institutions of Higher Learning, the Young Top-Notch Talent Support Program of Shanghai, the Special Financial Grant from the China Postdoctoral Science Foundation (Grant No. 2016T90346) and 111 Project (No. B12024).

DATA AVAILABILITY

The data that support the findings of this study are available from the corresponding authors upon reasonable request.

REFERENCES

- 1P. Pringsheim, *Z. Phys.* **57**(11), 739 (1929).
- 2R. I. Epstein, M. I. Buchwald, B. C. Edwards, T. R. Gosnell, and C. E. Mungan, *Nature* **377**(6549), 500 (1995).
- 3S. Rostami, A. R. Albrecht, A. Volpi, M. P. Hehlen, M. Tonelli, and M. Sheik-Bahae, *Opt. Lett.* **44**(6), 1419 (2019).
- 4J. Fernandez, A. J. Garcia-Adeva, and R. Balda, *Phys. Rev. Lett.* **97**(3), 033001 (2006).
- 5S. Rostami, A. R. Albrecht, A. Volpi, and M. Sheik-Bahae, *Photonics Res.* **7**(4), 445 (2019).
- 6A. Volpi, G. Cittadino, A. D. Lieto, A. Cassanho, H. P. Jenssen, and M. Tonelli, *Opt. Eng.* **56**(1), 011105 (2016).
- 7B. Zhong, J. Yin, Y. Jia, L. Chen, Y. Hang, and J. Yin, *Opt. Lett.* **39**(9), 2747 (2014).
- 8G. Cittadino, A. Volpi, A. D. Lieto, and M. Tonelli, *Opt. Eng.* **56**(1), 011107 (2016).
- 9M. P. Hehlen, J. Meng, A. R. Albrecht, E. R. Lee, A. Gragossian, S. P. Love, C. E. Hamilton, R. I. Epstein, and M. Sheik-Bahae, *Light. Sci. Appl.* **7**(1), 15 (2018).
- 10S. D. Melgaard, A. R. Albrecht, M. P. Hehlen, and M. Sheik-Bahae, *Sci. Rep.* **6**(1), 20380 (2016).
- 11S. Bigotta, A. D. Lieto, D. Parisi, A. Toncelli, and M. Tonelli, *Proc. SPIE* **6461**, 64610E (2007).
- 12B. Zhong, H. Luo, Y. Shi, and J. Yin, *Opt. Eng.* **56**(1), 011102 (2016).
- 13A. Volpi, G. Cittadino, A. D. Lieto, and M. Tonelli, *J. Lumin.* **203**, 670 (2018).
- 14A. Mendioroz, J. Fernandez, M. Voda, M. Al-Saleh, R. Balda, and A. Garcia-Adeva, *Opt. Lett.* **27**(17), 1525 (2002).
- 15J. Fernández, R. Balda, M. Barredo-Zuriarrain, O. Merdrignac-Conanec, N. Hakmeh, S. Garcia-Revilla, and M. Arriandiaga, *Proc. of SPIE Vol. 9380*, 93800A-1-93800A-10 (2015).
- 16V. Babajanyan, *Laser Phys.* **23**(12), 126002 (2013).
- 17B. Zhong, Y. Lei, H. Luo, Y. Shi, T. Yang, and J. Yin, *J. Lumin.* **226**, 117472 (2020).
- 18G. Cittadino, E. Damiano, A. D. Lieto, and M. Tonelli, *Opt. Express* **28**(10), 14476 (2020).
- 19P. B. Roder, B. E. Smith, X. Zhou, M. J. Crane, and P. J. Pauzauskie, *Proc. Natl. Acad. Sci. U. S. A.* **112**(49), 15024 (2015).
- 20X. Zhou, B. E. Smith, P. B. Roder, and P. J. Pauzauskie, *Adv. Mater.* **28**(39), 8658 (2016).
- 21J. Zhang, D. Li, R. Chen, and Q. Xiong, *Nature* **493**(7433), 504 (2013).
- 22S.-T. Ha, C. Shen, J. Zhang, and Q. Xiong, *Nat. Photonics* **10**(2), 115 (2016).
- 23X. Xia, A. Pant, A. S. Ganas, F. Jelezko, and P. J. Pauzauskie, *Adv. Mater.* (published online, 2020).
- 24M. Sheik-Bahae and Z. Yang, *IEEE J. Quantum Electron.* **56**(1), 1 (2020).
- 25M. Peysokhan, E. Mobini, A. Allahverdi, B. Abaie, and A. Mafi, *Photonics Res.* **8**(2), 202 (2020).
- 26S. R. Bowman, S. P. O'Connor, S. Biswal, N. J. Condon, and A. Rosenberg, *IEEE J. Quantum Electron.* **46**(7), 1076 (2010).
- 27G. Nemova and R. Kashyap, *Opt. Commun.* **319**, 100 (2014).
- 28M. A. Ahmed, M. Haefner, M. Vogel, C. Pruss, A. Voss, W. Osten, and T. Graf, *Opt. Express* **19**(6), 5093 (2011).
- 29D. J. Richardson, J. Nilsson, and W. A. Clarkson, *J. Opt. Soc. Am. B* **27**(11), B63 (2010).
- 30M. Rumpel, A. Voss, M. Moeller, F. Habel, C. Moormann, M. Schacht, T. Graf, and M. A. Ahmed, *Opt. Lett.* **37**(20), 4188 (2012).
- 31C. Jauregui, J. Limpert, and A. Tünnermann, *Nat. Photonics* **7**(11), 861 (2013).
- 32W. Koechner, *Solid-State Laser Engineering* (Springer, New York, NY, 2006).
- 33S. Biswal, S. P. O'Connor, and S. R. Bowman, *Appl. Phys. Lett.* **89**(9), 091911 (2006).
- 34R. Epstein, J. Brown, B. Edwards, and A. Gibbs, *J. Appl. Phys.* **90**(9), 4815 (2001).
- 35Z. Yang, J. Meng, A. R. Albrecht, and M. Sheik-Bahae, *Opt. Express* **27**(2), 1392 (2019).
- 36E. S. d Lima Filho, G. Nemova, S. Loranger, and R. Kashyap, *Opt. Express* **21**(21), 24711 (2013).
- 37G. Nemova and R. Kashyap, *J. Opt. Soc. Am. B* **31**(2), 340 (2014).
- 38W. Zhao, G. Zhu, Y. Chen, B. Gu, M. Wang, and J. Dong, *Appl. Opt.* **57**(18), 5141 (2018).
- 39X. Guo, F. Zheng, C. Li, X. Yang, N. Li, S. Liu, J. Wei, X. Qiu, and Q. He, *Opt. Laser Eng.* **115**, 243 (2019).
- 40Y. Nakayama, Y. Harada, and T. Kita, *Opt. Express* **27**(24), 34961 (2019).
- 41K. R. Hansen, T. T. Alkeskjold, J. Broeng, and J. Lægsgaard, *Opt. Express* **19**(24), 23965 (2011).
- 42W. Liu, J. Cao, and J. Chen, *Opt. Express* **27**(6), 9164 (2019).
- 43I. Moshe, S. Jackel, and A. Meir, *Opt. Lett.* **28**(10), 807 (2003).
- 44H. Chi, C. M. Baumgarten, E. Jankowska, K. A. Dehne, G. Murray, A. R. Meadows, M. Berrill, B. A. Reagan, and J. J. Rocca, *J. Opt. Soc. Am. B* **36**(4), 1084 (2019).
- 45S. R. Bowman, S. P. O'Connor, and S. Biswal, *IEEE J. Quantum Electron.* **41**(12), 1510 (2005).
- 46S. R. Bowman, *IEEE J. Quantum Electron.* **35**(1), 115 (1999).
- 47Z. Yang, A. R. Albrecht, J. Meng, and M. Sheik-Bahae, "Radiation balanced thin disk lasers," in *Conference on Lasers and Electro-Optics, OSA Technical Digest* (online) (Optical Society of America, 2018), paper SM4N.5.
- 48L. Cheng, L. B. Andre, A. J. Salkeld, and S. C. Rand, "Saturation effects in laser cooling of crystals," in *Conference on Lasers and Electro-Optics, OSA Technical Digest* (Optical Society of America, 2019), paper STh4H.4.
- 49J. Czochralski, *Z. Phys. Chem.* **92U**(1), 219 (1918).
- 50D. V. Seletskiy, R. Epstein, and M. Sheik-Bahae, *Rep. Prog. Phys.* **79**(9), 096401 (2016).
- 51D. V. Seletskiy, S. D. Melgaard, S. Bigotta, A. D. Lieto, M. Tonelli, and M. Sheik-Bahae, *Nat. Photonics* **4**(3), 161 (2010).
- 52G. Nemova and R. Kashyap, *Rep. Prog. Phys.* **73**(8), 086501 (2010).
- 53D. V. Seletskiy, M. P. Hehlen, R. I. Epstein, and M. Sheik-Bahae, *Adv. Opt. Photonics* **4**(1), 78 (2012).